

Ameliorating Effect of Platelet - Rich Plasma on Histological and Biochemical Changes Induced by Bisphenol-A in Prostate of Adult Albino Rats

Original
Article

Nahla Ibrahim, Ayaa Elsadek, Assmaa Selim and Sally Selim

Department of Medical Histology and Cell Biology, Faculty of Medicine, Zagazig University, Egypt

ABSTRACT

Background: The incidence of male reproductive disorders has been increased and may be linked to the environmental natural and synthetic chemicals. These chemicals are known as endocrine disrupting chemicals (EDCs); Bisphenol-A (BPA) is the most common one. Platelet rich plasma (PRP) is an autogenous and economical source of growth factors which nowadays used in the tissue repair.

Aim of the Work: Evaluate the possible therapeutic effect of PRP against BPA induced prostatic lesions in adult albino rats.

Materials and Methods: Thirty five adult male albino rats were divided into 3 main groups. Group I served as control, Group II: the rats were received 50 mg/kg BPA once daily for 4 weeks, Group III: the rats were received BPA as group II then 0.5 ml of PRP subcutaneous injected twice weekly for 4 weeks. After 8 weeks, rats of all groups were subjected to the followings; biochemical analysis of serum testosterone, immunohistochemical studies for androgen and estrogen receptors (AR &ER), light and electron microscope examination.

Results: Serum testosterone levels showed a highly significant decrease in group II when compared to others. Histologically, BPA treated prostate showed abundant collagen fibers with congested blood vessels and inflammatory cellular infiltration while, their acini showed numerous folds with epithelial stratification. Ultrastructurally, the secretory cells had heterochromatic nuclei, dilated endoplasmic reticulum, apical few microvilli and polymorphic secretory granules with lysosomes. Nearly all acinar cells showed negative nuclear ARs while positive ERs detection in basal cells. After PRP administration, showed improvement of many of these changes.

Conclusion: Exposure to BPA at low dose induced deleterious effects on the histological structure of the prostate and disturbed reproductive hormones. PRP showed significant signs of restoration of these changes.

Received: 11 January 2021, **Accepted:** 08 March 2021

Key Words: Biochemistry, bisphenol A prostate PRP histology, immunohistochemistry.

Corresponding Author: Nahla Ibrahim, MD, Department of Medical Histology and Cell Biology, Faculty of Medicine, Zagazig University, Egypt, **Tel.:** +20 11111 59033, **E-mail:** nona1811@yahoo.com

ISSN: 1110-0559, Vol. 45, No.1

INTRODUCTION

The prostate is the largest accessory gland in the reproductive system of male. It secretes a slightly alkaline fluid that appears to contain about one third of the seminal fluid in human. The development and function of the prostate is dependent on androgens produced mainly in the testes^[1]. The rodent prostate has a complicated system consisting of ventricular, lateral, dorsal and anterior lobes. While most studies have focused on the ventral prostate (VP), this lobe does not align the primates, while the dorsolateral prostatic lobe (DLP) is histologically same to the human. Also, DLP was more sensitive to low-dose bisphenol A (BPA) compared with the VP and it might be homologous with the peripheral or transitional zones and human benign prostatic hyperplasia (BPH) originated in these zones^[2].

Gradually, the incidence of male reproductive disorders has been increased and these disorders may be correlated with organic and inorganic chemicals in the environment. These chemicals are well known as endocrine disrupting chemicals (EDCs)^[3].

Bisphenol-A (BPA) is an EDC used in the manufacture of polycarbonate plastics and epoxy resins for the industrial treatment of water pipes and metal can liners. It is also present in some plastic food and beverage containers, all disposable plastics and some dental equipment and fillings^[4]. Thermal paper, as used in credit card receipt printers and other types of retail applications, represents an additional source of BPA. BPA can be transferred from heat-printed receipts in transient contact. Although the rate of skin penetration for BPA is unclear, a study indicated that these exposures were associated with significant increases

in unconjugated BPA in serum. Other sources of exposure include medical devices, mouthing of toys by children, cigarette filters, household detergents and personal care products. Several studies have proven the existence of BPA in canned food^[5].

The health hazards of BPA are majorly due to an incomplete polymerization reaction which keeps some unbound BPA molecules in the products. These unbound molecules may leak into food or beverage over time, particularly under heat, acidic or basic environmental conditions^[6].

Exposure to BPA is linked to a range of health problems with a particular focus on male reproductive dysfunction. BPA acts as an agonist, antagonist, or modulator of several receptor hormones. It acts as antagonist to the androgens^[7]. It has an influential oestrogenic action. However, it has been verified to be anti-estrogen at higher doses^[8,9].

Platelet Rich-Plasma (PRP) is a biological outcome represented as a portion of the plasma fraction of autologous blood with a high platelet density above the base point. It encompasses not only a high level of platelets but also a full complement of clotting factors, chemokines, platelet-rich-fibrin (PRF) and other cytokines that alter the pericellular microenvironment and numerous different plasma proteins^[10].

In the 1970s the concept of PRP started in the field of human hematology which was used to treat thrombocytopenia. Thereafter, it has been used in a large scale in the musculoskeletal field as in sports injuries. Also, it is used in many medical and surgical fields such as pediatric, gynecology, dentistry, orthopedics, neurosurgery, cardiac surgery and cosmetic surgery^[11]. Moreover, the interest in its application in dermatology, tissue regeneration, wound healing, improvement of burn and alopecia has increased^[12,10]. The wide spread application of PRP would provide new hope for tissue repair rather than ineffectual medical and surgical treatment^[13].

So, this study aimed to clarify the structural changes that may occur in the DLP of albino rats after administration of Bisphenol –A and to evaluate the therapeutic effect of PRP.

MATERIAL&METHOD

Chemicals and preparation

1) Bisphenol A (BPA)

It is beige odorless white crystalline powder (purity >97%). Its CAS No was 80-05-7. It was manufactured by Sigma-Aldrich Chemical Company (St Louis, Missouri, USA) and purchased from Sigma-Egypt. It was dissolved in corn oil (vehicle).

Blood sampling and PRP preparation

Seven male rats were used for obtaining PRP. Its preparation was performed at the medical biochemistry department of Faculty of Medicine, Zagazig University. It was carried out by adapting the protocol of the double centrifugation tube method.

The PRP was prepared using the double centrifugation tube method. Fresh venous blood was collected from the jugular veins of healthy male rats 20 mL was collected into tubes contained citrate-dextrose-acid and at 1000g for 10 minutes. It was centrifuged to get PRP at the surface of the test tube. PRP was further centrifuged to obtain a platelet concentrate (PC) at 1500g for 10 minutes. The final product was 4.5 times platelets more than platelet-poor plasma and the baseline. The PC was kept in sterile tube and added human thrombin (0.2 ml /1mL PC) and calcium chloride (0.8mL PRP + 0.2mL 10% CaCl₂), immediately before injection to activate platelets to degranulate and release its own growth factors. The 20 ml of whole blood yields 2 ml PRP^[14,15].

Animals and experimental design

Thirty five healthy adult male albino rats with an average age of 12-14 weeks and body weight ranging from 180-200 grams were accustomed in this study. They were brought from the breeding animal house, Faculty of Medicine, Zagazig University. They were preserved in the animal house for seven days allowing them to habituate to the new environment before the experiment. Throughout the duration of the experiment, the rats were housed in clean stainless steel cages and kept under the same environmental conditions regarding light, feeding and temperature. They were allowed ad-libitum access to food and water. All rats received human care in compliance with the guidelines of the Medical Research Ethics Committee of Zagazig University, Egypt (The protocol approval number was ZU-IACUC/3/F/55/2019) and was conformed to the National Institutes of Health guide for the care and use of laboratory animals.

These rats were randomly divided into three main groups:

Group I (Control group): Included twenty one rats were equally subdivided into three subgroups (seven rats each).

Subgroup IA (negative control subgroup): The rats received only regular diet and water for 8 weeks.

Subgroup IB (vehicle corn oil subgroup): The rats received 0.5ml of corn oil (the vehicle of BPA) by oral gavage once daily for 8 weeks.

Subgroup IC (vehicle phosphate buffer saline subgroup): The rats were received twice weekly subcutaneous injections of phosphate buffer saline (PBS) (the vehicle of PRP) at a dose of 0.5 ml for 8 weeks.

Group II (BPA treated): (Included seven rats) the rats received 50 mg/kg BPA dissolved in 0.5ml corn oil by oral gavage once daily^[16] for 4 weeks^[17].

Group III (BPA & PRP treated): (Included seven rats) the rats received BPA as group II then 0.5 ml of PRP which was dissolved in PBS (1:1) immediately aspirated with micropipette, placed in a sterile insulin syringe and injected subcutaneously twice weekly for 4 weeks^[18].

At the end of the experiment, at designated time, (after 8 weeks) rats of all groups were weighed and these body weights were recorded for statistical analysis, then all rats were subjected to the followings methods.

Biochemical analysis

The rats were anaesthetized by ether inhalation. Venous blood samples were obtained by means of capillary glass tubes from the retro-orbital plexus. This blood samples were used for biochemical analysis and were collected at a fixed time of the day to minimize the diurnal variation^[19]. Total serum testosterone hormone in samples were assessed by an enzyme-linked immunosorbent assay (ELISA). Kit used was The BioVendor rat/mouse Testosterone ELISA Kit (IB79174, IBL-America, Minneapolis, Minnesota, USA), measured by ELISA reader.

Intra-cardiac perfusion was carried out through the heart apex with 300 ml of 2.5% glutaraldehyde in 0.1 mol/l cacodylate buffer (pH 7.3) for 5 min for partial fixation of the prostates. A midline lower abdominal incision was performed to expose the urogenital complex. The prostate glands were taken out and weighted. The right dorsolateral prostatic lobes were dissected and immediately processed for histological study.

Histological study

Specimens for light microscope examination the right dorsolateral lobe of the prostate (DLP) were bisected into two longitudinal halves; one half was immediately immersed in 10% formal saline for 48 h and were processed to prepare 5- μ m thick paraffin sections for hematoxyline and eosin, Mallory Trichrome and immunohistochemical stains^[20].

The other half was cut into 1mm³ slices and processed for transmission electron microscopic examination. Specimens were immediately fixed in the same perfusion fixative (2.5% glutaraldehyde) for 2h and postfixed in 1% osmium tetroxide buffered with 0.1M phosphate buffer at pH 7.4 for 1h. Then, they were dehydrated in ascending grades of alcohol and embedded in resin to prepare semithin and ultrathin sections using a Leica ultracut (Glienicke, Berlin, Germany). Semithin sections (1- μ m-thick) were stained with 1% toluidine blue for light microscopic examination. Ultrathin sections were stained with uranyl acetate and lead citrate^[21,20]. The prepared sections were examined and photographed by JEOL JEM 1010 transmission electron microscope in Electron Microscope Research Laboratory Unit, Faculty of Agriculture, Mansoura University.

Immunohistochemical study

Immunohistochemical reaction was carried for identification of nuclear androgen (AR) and estrogen (ER) receptors which appear as nuclear brown coloration using avidin biotin peroxidase system. The primary antibody (nuclear AR and ER) used was a mouse monoclonal antibody of IgG immunoglobulin type (Dako Life Trade -Egypt, clone 1A4, code No. M0851). It was obtained

from Sigma Biochemical (St. Louis, Missouri, USA). The antigen was finally tracked down by the addition of DAB Chromogen. Slides were counterstained with Mayer's haematoxylin. The negative control sections from prostate were processed in the same way but without primary antibodies addition. Positive control was testis according to the kit^[22].

Image analysis and morphometric studies

Epithelial height, area percent of collagen and number of positive nuclear AR & ER immunorexpression were assessed by an ordinary light microscope using Leica 500 image analyzer computer system (England) at the Image Analyzing Unit of the Pathology Department, Faculty of Dentistry, Cairo University, Egypt. The procedure was performed using H&E, Mallory trichrome, immunohistochemical stained sections at a total magnification of $\times 400$ by measuring 10 non-overlapping fields from each specimen of randomly chosen five rats of each group.

Statistical analysis

The data obtained from all groups (body and prostate weights, serum testosterone level as well as epithelial heights and number of positive nuclear immunorexpression of both AR & ER) were expressed as mean \pm standard deviation (\pm SD). These data were subjected to statistical analysis using Statistical Package for the Social Sciences (SPSS) program version 20. Statistically significant difference was determined by one way analysis of variance (ANOVA). ANOVA was statistically significant when *P value* <0.05, statistically highly significant when *P value* <0.001 and non-significant when *P*>0.05^[23].

RESULTS

Results obtained from all subgroups of group I regarding body and prostate weights, hormonal analysis, light with electron microscope studies and morphometrical analysis were similar. So we use the results of subgroup Ia to express the control.

Body and prostate weights

The body weights showed no statistically significant difference in group II when compared to other groups (*P*>0.05) and also no difference between groups I and III (*P*>0.05) (Table 1).

Prostatic weights showed a highly statistically significant decrease in group II when compared to other groups (*P*<0.001) while there was no difference between group I and group III (*P*>0.05) (Table 2)

Biochemical analysis

Serum testosterone levels showed a highly statistically decrease in group II when compared to others (*P*<0.001), while there was no difference between groups I and III (*P*>0.05) (Table 3).

Histological results

H&E stained specimens obtained from all control subgroups (Group I) showed the same normal histological structure of right DLP. Closely packed secretory acini of nearly regular sizes and shapes, few mucosal folds and homogenous acidophilic secretions fill their lumina were observed. Minimal interacinar spaces with sparse stroma were noticed. Acini were lined by simple cuboidal to columnar epithelium with rounded to oval basal nuclei with prominent nucleoli. Blood vessels were noticed in the interacinar stroma (Figures 1A,2 A). BPA treated group (II) revealed some alterations in the histological structure of the acini and stroma. Disturbance of sizes and shapes of some secretory acini with wide some interacinar spaces (Figure 1B). Some acini were lined by columnar epithelium with a focal area of stratification; numerous basal cells with darkly stained flat nuclei were noticed with separation from the above luminal epithelium (Figure 2B). Numerous mucosal folds and luminal secretions of variable densities, pale, acidophilic and vacuolated were seen. (Figures 1B,2B). Other acini showed flattening of the epithelial lining in some areas and luminal pale acidophilic secretions with wide interacinar space (Figure 2C). Intraepithelial inflammatory cells and numerous mast cells were noticed (Figure 2D). Other acini revealed marked inflammatory cellular infiltration and congested blood vessels (Figure 2E). Focal areas of stratification were also seen (Figures 2D,2E). Concerning group III administration of PRP to BPA treated rats revealed partially preserved most of the epithelial and stromal structures. Nearly normal architecture of prostatic acini but some secretory acini with few mucosal folds and sparse stroma were observed in narrow interacinar spaces (Figure 1C). Small focal areas of stratification were also noticed (Figure 2F). Homogenous acidophilic secretions fill their lumina were seen (Figures 1C,2F).

Mallory's trichrome-stained sections of group I showed minimal amount of collagen fibers in the interacinar stroma and around the acini (Figure 3A). While, group II revealed abundant collagen fibers in the stroma and around congested blood vessels (Figure 3B). Group III had minimal amount of collagen fibers in the stroma and around blood vessel (Figure 3C).

Regarding Immunoperoxidase technique for AR. Group I revealed a strong nuclear reaction of ARs nearly in all luminal acinar epithelial cells (Figure 4A). While, group II showed few acinar cells with positive ARs nuclear immunoreaction while, all others with negative reaction (Figure 4B). Most of acinar cells in group III appeared with positive ARs nuclear reaction while, some cells with negative reaction (Figure 4C).

Concerning Immunoperoxidase technique for ER, Positive ERs immunoreaction localized in the basal cells nuclei of acini in group I were observed (Figure 5A). Group II revealed a strong positive immunoreaction in the nuclei of numerous basal cells of acini (Figure 5B).

A positive immunoreaction in the nuclei of some basal cells were seen in group III (Figure 5C).

Results of Toluidine blue stained semithin sections from right DLP of group I revealed columnar cells with apical pale vacuolated cytoplasm and basal rounded to oval vesicular nuclei. Flat or trigonal basal cells with darkly stained nuclei, interacinar stroma with smooth muscle cells and blood capillaries were seen (Figure 6A). In group II epithelial cells showed separation from the underlying thick irregular basement membrane and basal cells with flat or elongated darkly stained nuclei (Figure 6B). A part of acini with stratified epithelium revealed some detached cells with irregular nuclei or cytoplasmic bodies (Figure 6C). Invading blood capillaries were observed (Figures 6B,6C). Stratified epithelial cells revealed basal cells with flat darkly stained nuclei. Interacinar stroma contained blood capillaries and smooth muscle fibers (Figure 6D). Different nuclear patterns vesicular, dark, irregular and apical vacuolated cytoplasm were seen (Figures 6A,6B,6C). Group III revealed acinar parts with columnar cells with irregular shaped vesicular nuclei and apical vacuolated cytoplasm. Also, basal cells with flat, elongated, trigonal darkly stained nuclei and invading blood capillary were identified. Other parts showed stratified epithelium with rounded vesicular nuclei and also basal cells. Interacinar spaces contained blood capillaries and smooth muscle fibers (Figure 6E).

Ultrastructural results from right DLP of group I showed a part of an acinar lining epithelial cells resting on a regular thin basal lamina with regular, rounded, basal euchromatic nuclei and apical crowded abundant microvilli. Apical numerous secretory granules with electron dense cores, prominent rough endoplasmic reticulum, dispersed mitochondria, and parts of smooth muscle fibers were noticed (Figure 7A). Group II revealed parts of an acinar lining epithelial cells resting on a regular thick basal lamina and columnar secretory cells with irregular basal heterochromatic nuclei, their apical parts showed scattered few microvilli. Intraepithelial inflammatory cells with pale cytoplasm were seen (Figure 7B). Other parts of acini revealed prominent smooth muscle fibers with their dense bodies and two cell types; tall columnar luminal and basal cells. The luminal cells had irregular basal heterochromatic nuclei and basal cells with indented flat heterochromatic nuclei were seen (Figure 7C). Parts of mucosal folds with stratified epithelial cells with irregular shaped heterochromatic nuclei with irregular arrangement cisternae of endoplasmic reticulum, apical polymorphic secretory granules; dense cores, dense granular cores, empty and numerous aggregated microvilli (Figure 7D). Parts of acinar epithelial cells with a focal areas of stratification with irregular shaped nuclei; rounded, oval, apoptotic (Figure 7E). Dilated cisternae of endoplasmic reticulum and few apical secretory granules with dense granular appearance were observed (Figures 7B,7C,7E). Polymorphic lysosomes were seen (Figures 7C,7E). Aggregated and dispersed mitochondria

(Figure 7D,7E) were identified. Group III showed parts of an acinar epithelial cells with a focal areas of stratification. Indented nuclei, apical aggregated microvilli with secretory granules having electron dense cores and others were empty and Prominent Golgi apparatus were identified. Smooth muscle fibers with their dense bodies and flat oval nuclei were observed (Figure 7F).

Image analysis and morphometric studies

The epithelial heights and area % of collagen fibers showed a highly significant increase in group II when

compared to others ($P < 0.001$) and there was no difference between groups I and III ($P > 0.005$) (Tables 4,5). Regarding statistical analysis of the number of positive nuclear ARs immunexpression showed a highly significant decrease in group II when compared to other groups ($P < 0.001$) and there was no difference between groups I and III ($P > 0.005$) (Table 6). Moreover, the number of positive nuclear ERs immunexpression showed a highly significant increase in group II when compared to others ($P < 0.001$) while there was no difference between groups I and III ($P > 0.05$) (Table 7).

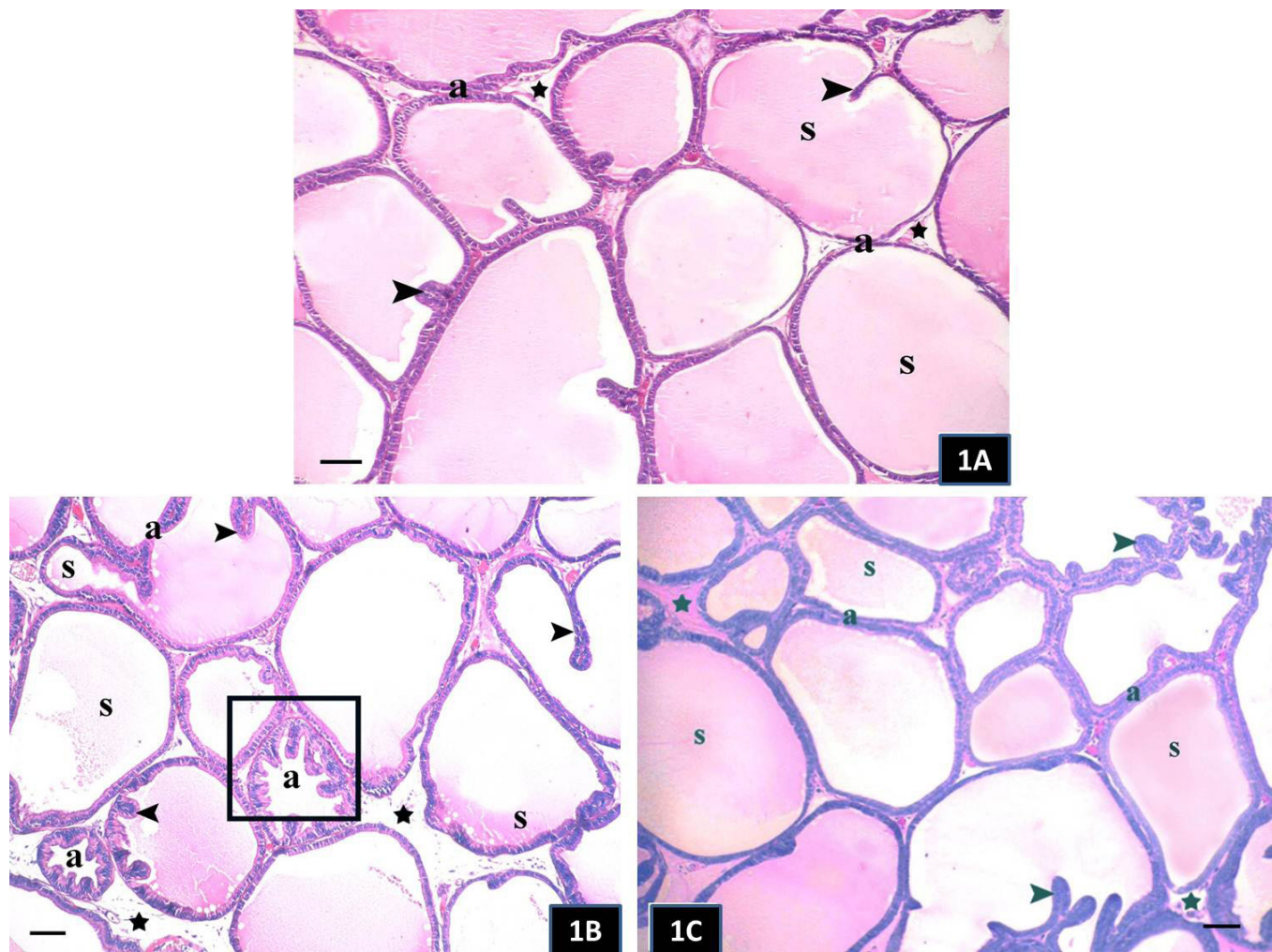


Fig. 1: H&E stained sections from right DLP of control group (A): showing closely packed secretory acini (a) of nearly regular sizes and shape, few mucosal folds (arrow head) and homogenous acidophilic secretions (s) fill their lumina are observed. Minimal interacinar spaces with sparse stroma (star) are noticed. Group II (B): Showing some secretory acini with disturbance of size and shape (a) and numerous mucosal folds (arrow head) are observed. Luminal secretions of variable densities, pale, acidophilic and vacuolated (s) are seen. Notice, wide some interacinar spaces (star). Group III (C): Nearly normal architecture of prostatic acini (a) but some secretory acini with few mucosal folds (arrow head) can be observed. Homogenous acidophilic and pale vacuolated secretions (s) are noticed fill the lumina of some acini. Sparse stroma (star) is observed in narrow interacinar spaces. (H&E $\times 100$, scale bar, 50 μ m)

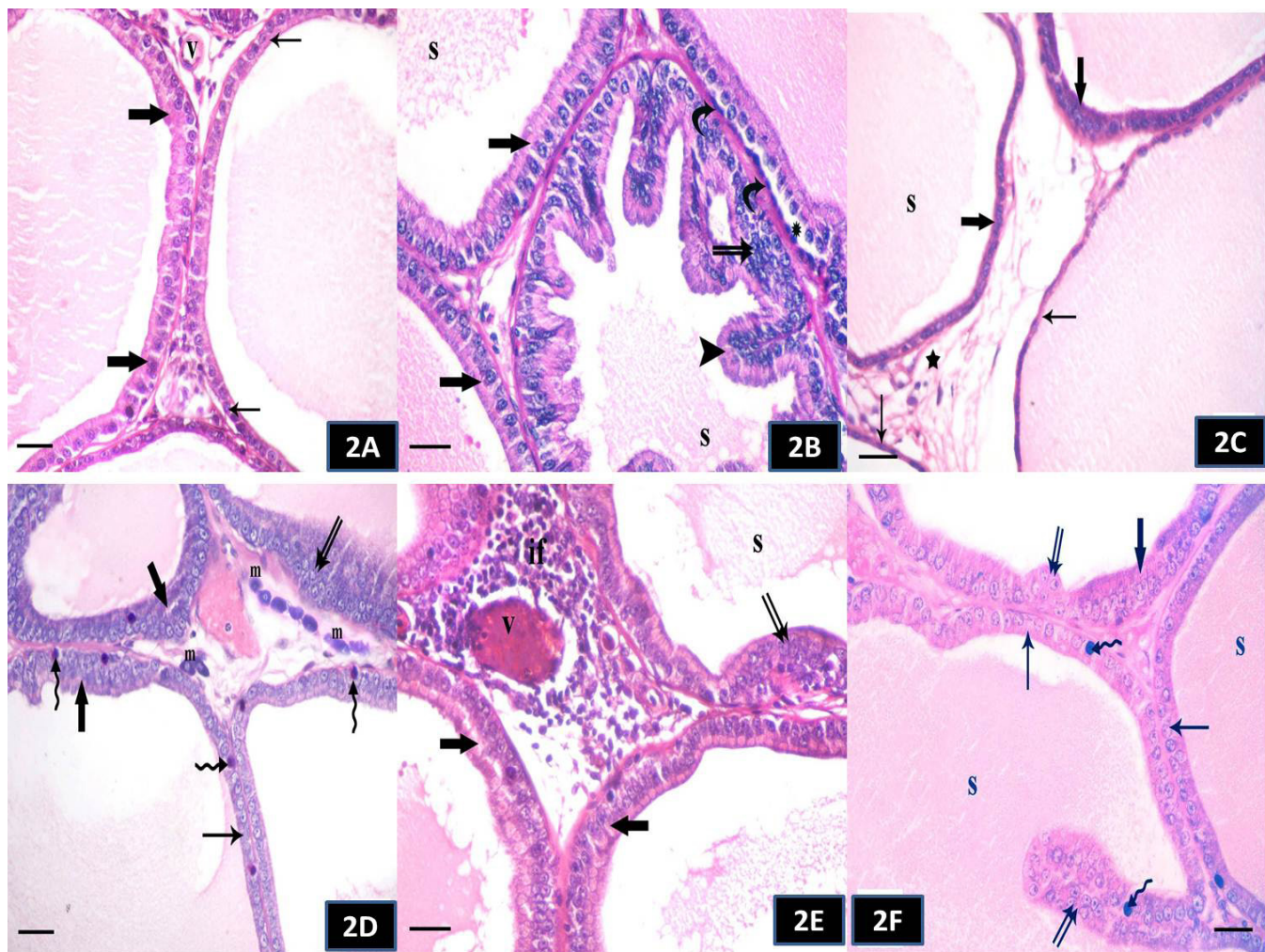


Fig. 2: H&E stained sections from right DLP of control group (A): showing acini lined by simple cuboidal (thin arrow) to columnar epithelium (thick arrow) with rounded to oval basal nuclei with prominent nucleoli are seen. Blood vessels (v) can be noticed in the interacinar stroma. While, group II (B,C,D,E). (B): Some acini are lined by columnar epithelium (thick arrow) and an acinus shows multiple mucosal folds (arrow head) with a focal area of stratification (double arrow). Numerous basal cells with darkly stained flat nuclei (curved arrow) can be noticed with separation from the above luminal epithelium (asterisk). Notice, luminal pale foamy or vacuolated acidophilic secretions (s). (C): Other acini are lined by cuboidal epithelium (thick arrow) and also show flattening of the epithelial lining in some areas (thin arrow). Notice, luminal pale acidophilic secretions (s) and wide interacinar space (star). (D): Acini are lined by tall columnar epithelium (thick arrow) and others by cuboidal epithelium (thin arrow) are seen. Focal area of stratification (double arrow), intraepithelial inflammatory cells (tailed arrow) and numerous mast cells (m) are noticed. (E): Acini with tall columnar epithelium (thick arrow) and others show a focal area of stratification (double arrow). Luminal vacuolated acidophilic secretions (s) are observed. Marked inflammatory cellular infiltration (if) and congested blood vessels (v) are seen. Group III (F): Reveals some acini lined by simple cuboidal epithelium with rounded nuclei (thin arrow) and others by columnar epithelium with basal oval nuclei (thick arrow). Small focal areas of stratification (double arrow) with intraepithelial inflammatory cells (tailed arrow) are noticed. Homogenous acidophilic secretions fill their lumina (s) (H&E $\times 400$, scale bar, $20\mu\text{m}$)

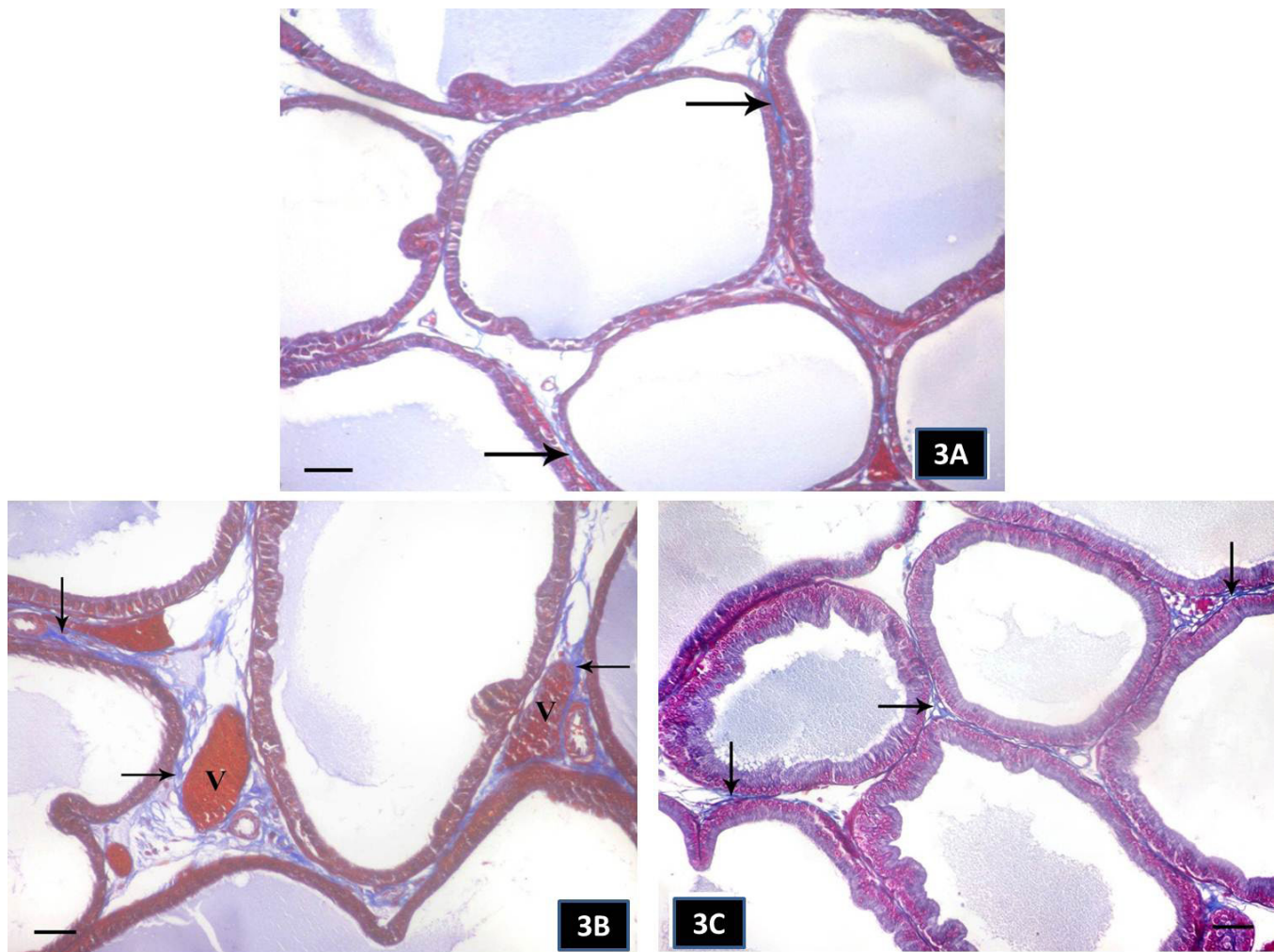


Fig. 3: (A):Mallory trichrome stained sections of the control group showing minimal amount of collagen fibers found in the interacinar stroma and around the acini. Group II (B): Abundant collagen fibers in the stroma and also around congested blood vessels (v) are seen. Group III (C): Reveals minimal amount of collagen fibers (arrow) in the stroma and also around blood vessel. (Mallory trichrome $\times 200$, scale bar, $30\mu\text{m}$)

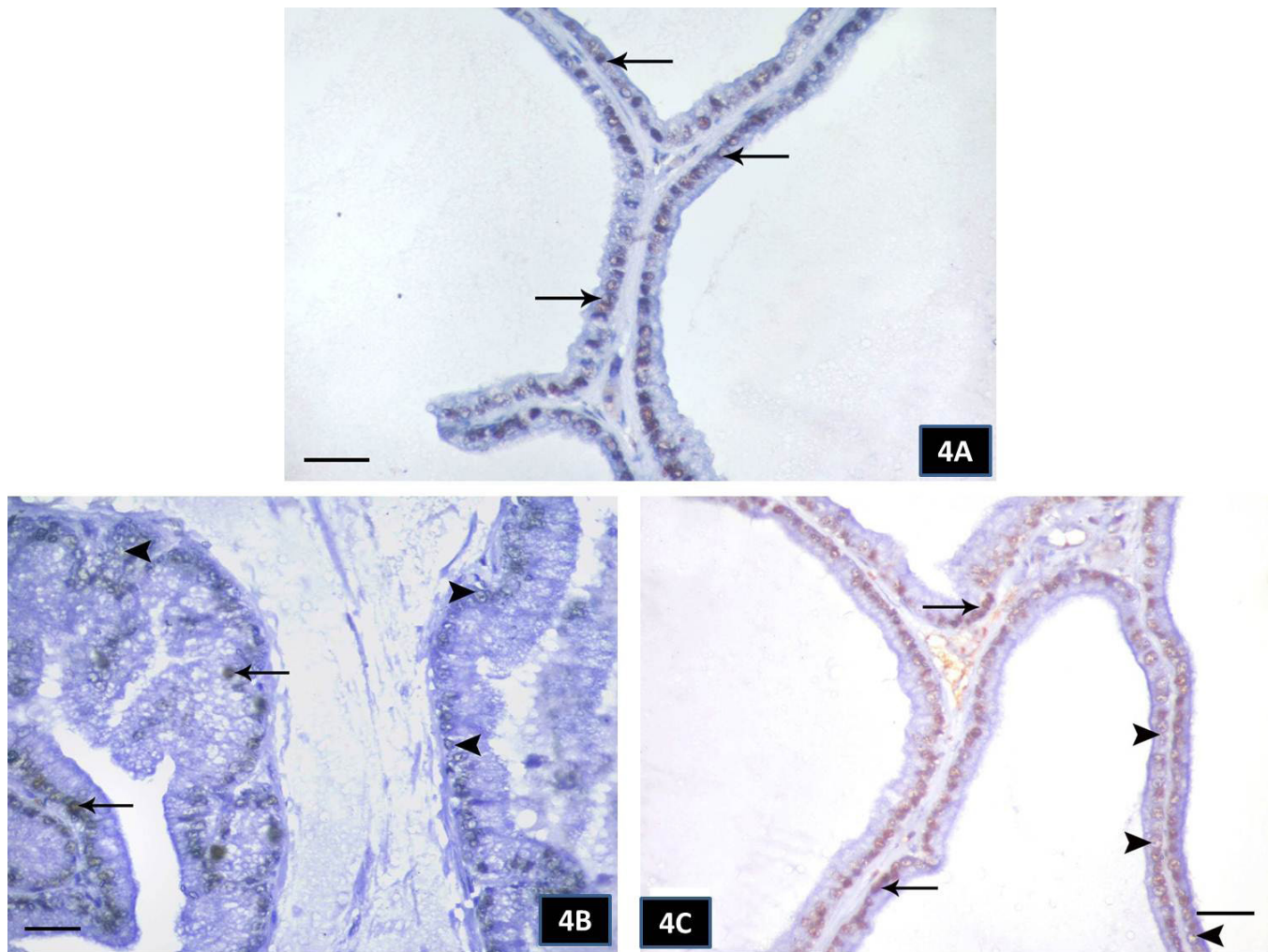


Fig. 4: (A):Immunohistochemical stained sectionsfor nuclear ARsfrom right DLP of control group showing a strong nuclear reaction of ARs nearly in all luminal acinar epithelial cells.Group II (B): Few acinar cells with positive ARs nuclear immunoreaction while, all others show negative reaction. Group III(C): Most of acinar cells with positive ARs nuclear reaction while, some cells show a negative reaction.(Immunoperoxidase technique for ARs x400, scale bar,20 μ m)

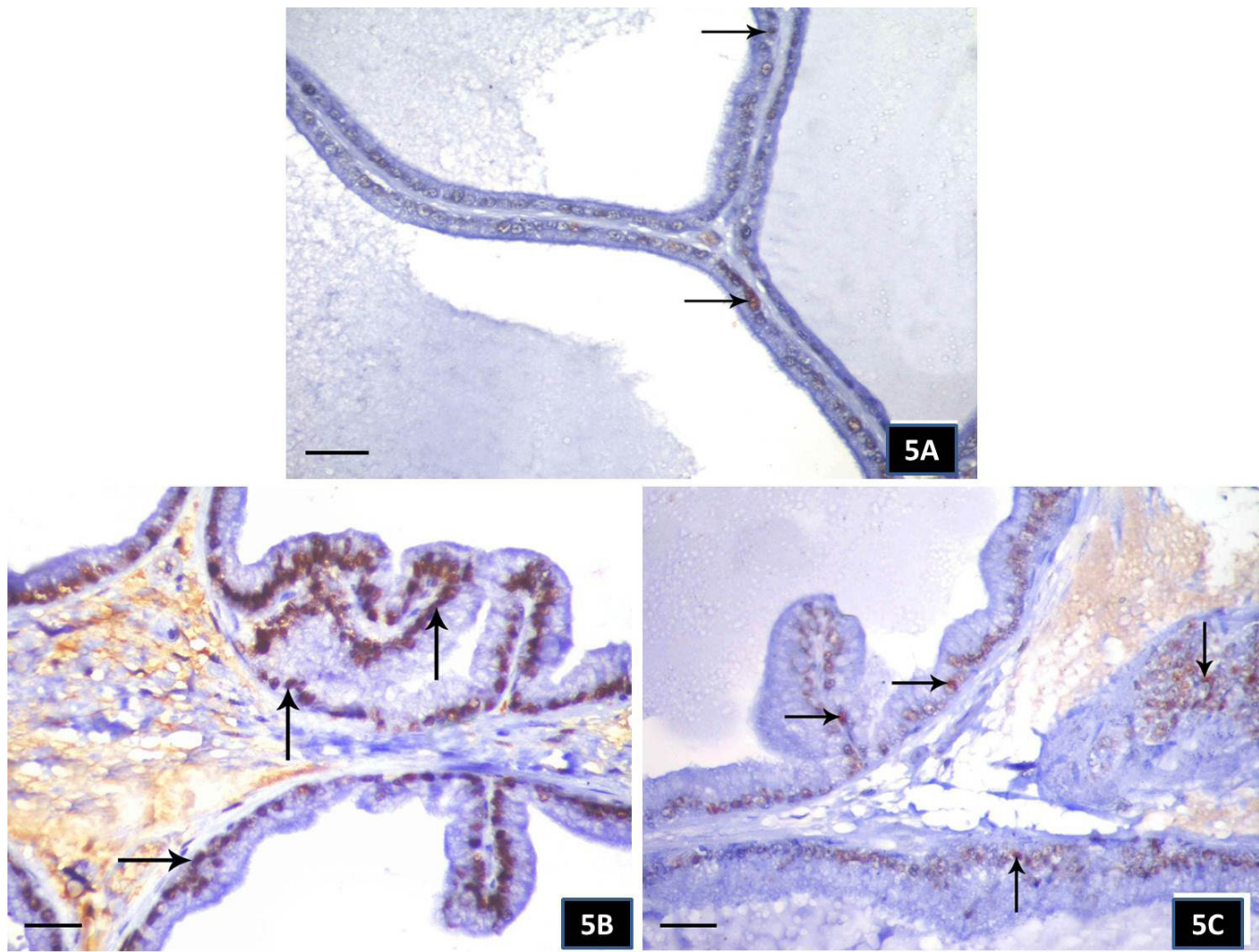


Fig. 5: (A):Immunohistochemical stained sectionsfor nuclear ERs from right DLP of control group showingpositive ERs immunorexpression localized in the basal cells nuclei of acini.Group II (B):reveals a strong positive immunorexpression in the nuclei of numerous basal cells of acini.In group III (C): A positive immunorexpression in the nuclei of some basal cells is seen..(Immunoperoxidase technique for ER, x400, scale bar, 20 μ m)

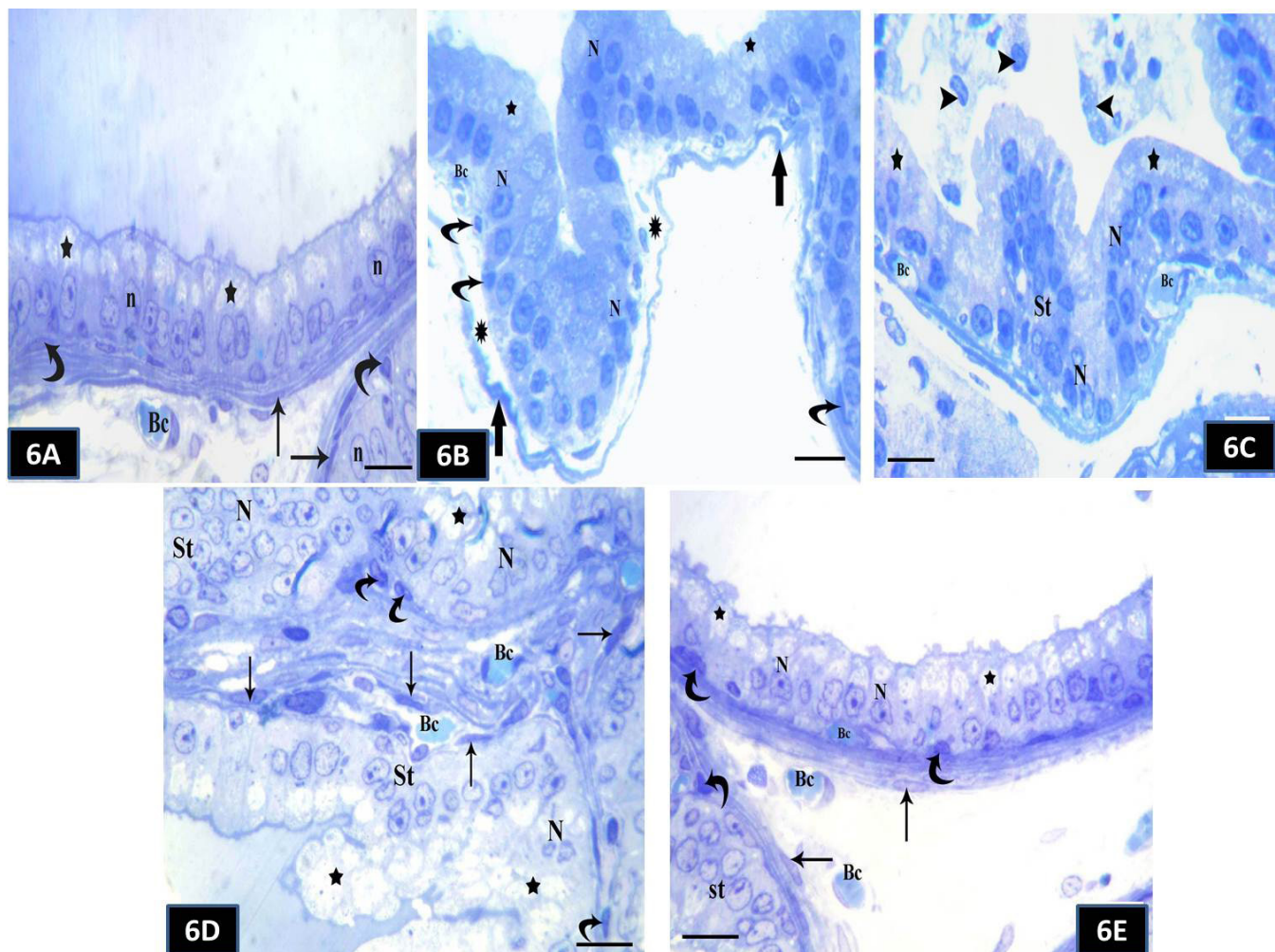


Fig. 6: Toluidine blue-stained semithin sections in right DLP of the control group (A): showing Columnar cells with apical pale vacuolated cytoplasm (star) and basal rounded to oval vesicular nuclei (n). Flat or trigonal basal cells with darkly stained nuclei (curved arrow) can be observed. Interacinar stroma shows smooth muscle cells (arrow) and blood capillary (Bc). Group II (B,C,D). (B): The epithelium is separated (asterisk) from the underlining thick irregular basement membrane (thick arrow). Columnar lining epithelium shows different nuclear patterns (N); vesicular, dark, irregular and apical vacuolated cytoplasm (star). Also, basal cells with flat or elongated darkly stained nuclei (curved arrow) are seen. Invading blood capillaries (Bc) can be observed. (C): A part of acinus shows stratified epithelium (St) with irregular shaped nuclei (N) and vacuolated cytoplasm (star). Some detached cells with irregular nuclei or cytoplasmic bodies (arrow head) are observed. Invading blood capillaries (Bc) can be also seen. (D): Stratified epithelium (St) shows irregular shaped nuclei (N) with extensive vacuolated cytoplasm (star). Also, basal cells with flat darkly stained nuclei (curved arrow) are well seen. Interacinar stroma contains blood capillaries (Bc) and smooth muscle fibers (arrow). In group III (E): An acinar part has columnar cells with irregular shaped vesicular nuclei (N) and apical vacuolated cytoplasm (star). Also, basal cells with flat, elongated, trigonal darkly stained nuclei (curved arrow) and invading blood capillary (Bc) are identified. Other part shows stratified epithelium (St) with rounded vesicular nuclei and also basal cells. Interacinar space contains blood capillaries (Bc) and smooth muscle fibers (arrow). (Toluidine blue x1000, scale bar, 10µm)

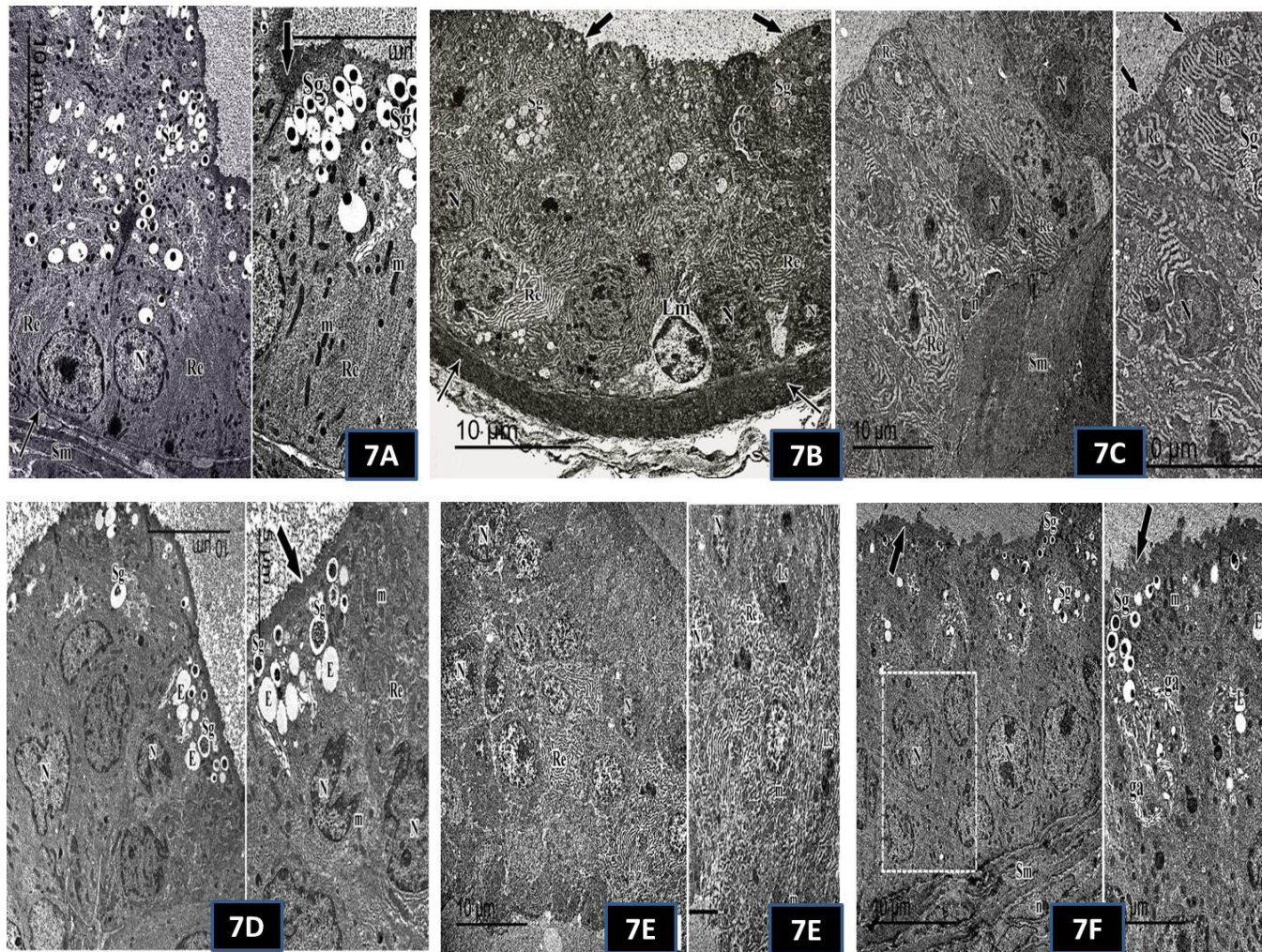


Fig. 7: Electron micrographs from right DLP of the control group(A): showing a part of an acinus lining epithelium resting on a regular thin basal lamina (thin arrow). It shows regular, rounded, basal euchromatic nuclei (N) and apical crowded abundant microvilli (thick arrow). Apical numerous secretory granules with electron dense cores (Sg), prominent rough endoplasmic reticulum (Re) and dispersed mitochondria (m) are also seen. A part of smooth muscle fibers (Sm) is noticed.

Group II (B,C,D,E). (B): A part of an acinus lining epithelium resting on a regular thick basal lamina (thin arrow). The columnar secretory cells have irregular basal heterochromatic nuclei (N) and mildly dilated cisternae of rough endoplasmic reticulum (Re). Their apical parts show scattered few microvilli (thick arrow) and secretory granules with dense granular appearance (Sg). Noticed, intraepithelial inflammatory cell with pale cytoplasm (Lm). (C): Other part of an acinus lining epithelium with prominent smooth muscle fibers with their dense bodies (Sm). It shows two cell types; tall columnar luminal and basal cells. The luminal cells have irregular basal heterochromatic nuclei (N), extensive dilated cisternae of endoplasmic reticulum (Re), few apical secretory granules with dense granular appearance (Sg) and polymorphic lysosomes (Ls). A basal one with indented flat heterochromatic nucleus (n) is well seen. (D): A part of mucosal fold with stratified epithelium. Its cells have irregular shaped heterochromatic nuclei (N) with irregular arrangement cisternae of endoplasmic reticulum (Re). Apical secretory granules; dense cores, dense granular cores (Sg), empty (E) numerous aggregated microvilli (arrow) and aggregated, dispersed mitochondria (m) can be observed. (E): A part of an acinus epithelium with a focal area of stratification. Its cells have irregular shaped nuclei; rounded, oval, apoptotic (N), dilated cisternae of endoplasmic reticulum (Re), aggregated mitochondria (m) and polymorphic lysosomes (Ls) Group III (F): Reveals a part of an acinus epithelium with a focal area of stratification (square). Indented nuclei (N), apical aggregated microvilli (thick arrow) with secretory granules having electron dense cores (Sg) and others are empty (E) and Prominent Golgi apparatus (ga) are identified. Smooth muscle fibers with their dense bodies (Sm) and flat oval nuclei (n) are observed (TEM).

Table 1: Comparison between the body weights of the different groups

Body weight (g)	Group I	Group II	Group III	<i>P Value</i>
Min.-Max.	196.73-204.65	193.85-204.55	191.12-200.28	0.100
Mean± S.D	200.833±3.048	199.054±3.939	196.631±3.279	

Table 2: Comparison between the Prostate weights of the different groups

Prostate weight (g)	Group I	Group II	Group III	<i>P Value</i>
Min.-Max.	6.58-8.05	6.23-7.05	7.30-7.94	<0.001*
Mean± S.D	7.577±0.486	6.669±0.286	7.643±0.235	

Table 3: Comparison between the Serum testosterone levels of the different groups

Serum testosterone level (ng/ml)	Group I	Group II	Group III	<i>P Value</i>
Min.-Max.	5.57-7.46	2.75-3.79	5.28-7.55	<0.001*
Mean± S.D	6.041±0.387	3.087±0.341	5.854±0.584	

Table 4: Comparison between the epithelial heights of the different groups

epithelial heights	Group I	Group II	Group III	<i>P Value</i>
Min.-Max.	48.20-55.09	67.56-74.81	51.42-58.50	<0.001*
Mean± S.D	51.3±4.762	71.543±2.390	54.59±2.321	

Table 5: Comparison between the Area % of collagen fibers of the different groups

Area % of collagen fibers	Group I	Group II	Group III	<i>P Value</i>
Min.-Max.	12.9-14.3	30.12-39.44	11.25-13.22	<0.001*
Mean± S.D	11.4±1.4	34.033±3.398	12.36±0.788	

Table 6: Comparison between the number positive nuclear ARs immunoeexpression of the different groups

Number of positive nuclear reaction	Group I	Group II	Group III	<i>P Value</i>
Min.-Max.	35-50	11-16	37-48	<0.001*
Mean± S.D	41.14±5.080	13.57±1.718	42.1 ±3.718	

Table 7: Comparison between the number positive nuclear ERs immunoeexpression of the different groups

Number of positive nuclear reaction	Group I	Group II	Group III	<i>P Value</i>
Min.-Max.	6-7	20-24	8-11	<0.001*
Mean± S.D	5.4±3.52	21.3±1.4	7.2 ± 2.91	

DISCUSSION

Owing to its pervasive existence in daily life, EDCs have recently attracted interest from the reproductive science community. Thus, reproductive disorders caused by EDCs are more common nowadays with regard to male infertility. These disruptors with adverse effects in adulthood are also vulnerable to male accessory sex glands^[24], but little is known about its effects on prostate. Also, BPA (as one of these EDCs) effects and mechanisms on reproductive system still remain unclear.

Hyperplasia involves common prostatic disorders. Surgical procedures with medical treatments are acceptable, but not totally effective or free of complications. Therefore, it is of vital importance to find a new method for treating prostatic diseases. A new hope can be offered by the evolving PRP sector^[13].

So, the present experimental study was designed to use a histological and biochemical approaches for evaluating the possible therapeutic effect of PRP against BPA induced prostatic changes in adult albino rats.

In the present work, BPA did not have a substantial effect on weight of the body. This result was in agreement with other researchers,^[25] who observed no substantial difference in rats' body weight, when exposed to BPA. On the other hand, body weight reduction was noticed by^[26], who explained it by metabolic activity disruption. While,^[27] stated that BPA has an estrogenic action that induces release of growth hormone and activates differentiation of adipocytes, observed body weight increase.

Regarding the prostatic weight,^[28,29] explained this decrease with regard to prostatic weight by the fact that the prostate size and functions are primarily dependent on the amount of testosterone that decreased following affection of Leydig cells. They found that the low dose of BPA reduced the weight of the testis, sperm count and germ cells. They attributed this to failed spermatogenesis by decreasing testosterone that stops meiosis of germ cells and activates the pathway of Fas/FasL that encourages their apoptosis. On the contrary,^[30] documented the selective effect of BPA on the prostate lobes and its biological effects modified with the dose. The pattern, however, was to increase the weight of the DLP in a dose-dependent manner. However, a direct correlation between its low dose and the prostate has not yet been identified.

In the present study, there was a highly significant decrease in serum testosterone level in BPA-treated group. This result was in accordance with^[31], who discovered that BPA could inhibit testosterone output by Leydig cells by reducing expression of both steroidogenic enzymes and steroidogenic acute regulatory (StAR) protein in a dose-related manner. In addition,^[6] found that BPA decreases testosterone production and secretion by modifying the hypothalamic-pituitary-testicular axis and inhibiting the activity of gonadotropic releasing hormone (GnRH) neurons, A large histological variation in DLP was observed

in rats treated with BPA. Similar results were observed by^[32,33], who assumed that BPA caused organ affection and toxicity by reducing the activity of antioxidant enzymes with elevated nitric oxide (NO) and malondialdehyde levels (MDA). The hypothesis that BPA also causes antioxidant depletion, oxidative stress and the release of free radicals is defined in this observation. The inflammatory cellular infiltration was mediated by those radicals. In addition, blood vessel dilation and congestion are components of the inflammatory response, bringing more blood to the degenerative or fibrosed areas. In addition,^[34] reported that nuclear factor-kappa- β (NF- κ B) could also be stimulated by these radicals. This pathway controls the development of pro-inflammatory cytokines and the recruitment of inflammatory cells that also contribute to the inflammatory response.

Mast cells with blood capillaries heavily invading the basement membrane have been documented in the current research. These findings were in line with^[35] who referred this to other mediators such as stem cell, VEGF and FGF variables that could cause mast cell chemotactic migration to vascularization sites. Invasive capillaries are a complex phenomenon that begins with tryptases, Mast cell proteases 6 and 7 which play an important role in angiogenesis and can act directly by cellular tryptase degradation of the basement membrane so allowing endothelial cells to penetrate, migrate and then proliferate. They also found that degranulation and activation of mast cells were associated with neovascularization.

This study demonstrated a statistically significant increase in the percentage of the collagen in the stroma. This finding coincided with^[36], who reported that mast cells are a key player in the process of inflammation and fibrosis control and induction through toll-like signalling of receptor-4 and increased pro-inflammatory cytokine production. A sequel to this, TGF- β 1 with a range of cytokines continues to be considered the key to fibrosis. They can drive fibroblast into myofibroblast proliferation and differentiation. In addition,^[37] documented myocardial fibrosis as a result of increased fibroblast proliferation and activation of mast cells. More recently,^[38] discovered that after BPA exposure, extensive thyroid fibrosis, referred this to increase in the number of mast cells which may be attributed to increased lipid peroxidation and reduced enzymatic activity of antioxidants.

The secretory acini showed flattening of their lining epithelium in the current work; this finding was in accordance with^[28] who discovered that germ cell numbers and sperm count were substantially reduced^[39]. have recorded a similar substantial decrease in the height of epididymis epithelial cells and adult rat seminiferous tubules after BPA exposure, respectively. Both of these, explained this by low testosterone levels.

In addition, in this study, numerous basal, intraepithelial inflammatory cells, elevated columnar epithelium, focal areas of stratification or proliferation and also numerous

prostatic epithelial infolding were observed in other acini in this sample. These results were in line with^[40], who reported that 80 percent of prostatic inflammatory cells consist of T-lymphocytes. Through the modulation of the various signaling pathways, infiltrating intraepithelial lymphocytes could encourage proliferation in a low androgen state. Also,^[30] revealed that BPA was able to cause DLP hyperplasia which was shown by increases in epithelial height and expression of proliferating cell nuclear antigen (PCNA).

Also,^[41] studied the crosstalk between mast cells and BPH. They found that BPH could increase the migration of mast cells and induce their activation. Conversely, cytokine IL-6 derived from mast cells promotes BPH through signalling pathways. Signal transducer & transcription activator (STAT), as well as extracellular signal-regulated kinase (ERK), mitogen-activated protein kinase (MAPK) and cyclin D1 are the most important routes. Such methods have an effect on cell formation, proliferation and differentiation. This newly identified signalling, preventing or interrupting mast cell migration will help us select better therapeutic strategies for BPH patients.

Nuclear pattern changes have been identified in the current research were in accordance with^[42], who referred these results to oxidative stress and lipid peroxidation as a result of BPA exposure. Lipid peroxidation subsequently stimulates endonuclease enzymes and interacts with DNA, causing DNA damage or break. Furthermore,^[43] stated that BPA induced comparable apoptosis by increasing cytosolic Ca₂, decreasing the transmembrane mitochondrial potential and increasing Polymerase-1 cleavage activities.

Noted sloughing of these cells in conjunction with cytoplasmic vacuolations and cellular detachment^[44], which could be correlated with changed intercellular adhesion molecule expression, cadherin-10, which is an important marker for luminal acinar cells. In addition,^[45] stated that a cellular defense mechanism against injurious substances may be possible. These dangerous substances have been isolated and blocked from interfering with cellular metabolism in vacuoles. Cellular detachment, on the other hand, is one of the key cell loss mechanisms involved in homeostatic cell size regulation. Terminal differentiation and orderly loss of dying cells compensated by cell renewal are closely correlated with this process.

Other observations were found by the electron microscope, although some of the secretory cells had hyperactivity symptoms, others with hypo-functions. Similar findings were obtained by^[46], who stated that the organelles involved in their secretory phase were mainly influenced by changes after exposure to BPA.

The thickening of basal laminain this study was in agreement with^[47] mwho explained the thickening of glomerular basement membrane by oxidative stress, production of inflammatory cytokines and growth factors lead to increased secretion of constitutional extracellular matrix components of the GBM, excessive collagen type

IV deposition and decrease of excess extracellular matrix degradation in diabetic nephropathy. While, in relation to increased lysosomal observation,^[48] found that lysosomal number, composition and function are sensitive to various external and internal stresses including oxidative stress, the key mechanism of BPA-induced degenerative lesions, which led to an increase in lysosome numbers as well as lysosomal activity.

With regard to dilated endoplasmic reticulum,^[49] reported that dilated reticulum in combination with other cellular changes is obviously confirmation of protein synthesis disruption. In addition, changes in the development of proteins within dilated cisternae may block the synthesizing of inhibitors of apoptosis such as Bcl-2 and/or the loss of proteins necessary for cell homeostasis, leading to its degeneration.

Regarding to the few acinar cells with positive nuclear ARs immunohistochemical finding was concomitant with^[50] who postulated that BPA antagonises AR activity through androgen binding rivalry, decreases AR movement from cytoplasm into the nucleus and prevents the formation of functional complexes that are the prerequisite for transcription, leading to transcription disruption and androgen-independent cell proliferation. On the other hand,^[30] found that, the expression of AR steadily increased with the rise in BPA dose. There is a debate as to whether AR terms are up-regulated or down-regulated. Therefore, the molecular processes of BPA on AR require more advanced explanation and clarification.

Whereas, strong positive ER immunoexpression in the nuclei of numerous basal cells of acini was in accordance with^[51], who confirmed that BPA functions as a xenoestrogen. Thus, the ER number and gene activity may be altered by BPA and interfere with hormone synthesis and clearance as well. This induces an imbalance in internal levels of androgen/estrogen. Also,^[30] and^[2] stated that the combination of BPA with ER led to an increase in the ER expression, which correspondingly promoted cell proliferation with exposure to lower doses of BPA. In addition, they documented that BPA could increase estradiol (E2) and decrease levels of testosterone lead to significant increase in the serum E2/T ratio, which was more pronounced at the high dose of BPA. This result was close to the hormone level shift in the elderly and caused BPH.

In the current study, PRP administration resulted in improvement of the histological and biochemical changes that observed in the BPA treated group. These findings were consistent with research in other organs previously recorded^[18]. found evidence of the regeneration of the diabetic pancreatic islet and exocrine part. In addition, PRP could position the pancreas in an environment that is similar to postnatal growth, where new lobules have been developed. Furthermore,^[52] found that in ischemia, PRP has been shown to exert a protective effect. Moreover,^[15] reported that PRP markedly improved the

dimethylnitrosurea (DMN)-induced changes in liver enzymes followed by a major down-regulation of fibrosis and markers of inflammation.

In addition,^[53,10] showed that PRP offered substantial safety primarily through anti-oxidant, anti-apoptotic, anti-fibrotic and anti-inflammatory interventions in relation to PRP enhancement. So, it can significantly enhance the mean histopathological scores of epithelialization, apoptosis, inflammation and fibrosis. In the same line,^[54] noted that by inducing ROS, PRP protects against UV-related photo-aging that alters the oxidant enzymatic mechanism. PRP has been shown to maintain the dermal fibroblast of the mouse by reducing the accumulation of free radicals by increasing the activity of intracellular antioxidant enzymes, especially glutathione peroxidase (GPx).

In addition,^[52] stated that PRP acts as a regulatory messenger of apoptosis as it reduces the expression of kinase-1 (ASK-1) signal-regulating apoptosis, a typical member of the family of mitogen-activated protein 3 kinase (MAP3K). These MAP3K modules containing three protein kinases that are sequentially activated are main components of a sequence of pathways critical signal transduction that regulate cellular processes as proliferation, differentiation and cell death.

In addition, by producing endogenous anti-inflammatory factors and promoting the synthesis of other interleukins, integrins, chemokines and cytokines,^[55] suggested that PRP could play a role as an anti-inflammatory agent^[56] indicated by other mechanisms that PRP inhibited excessive deposition of collagen, indicating that PRP could decrease fibrosis progression in damaged endometrium.

The antibacterial and analgesic effects of PRP have also been highlighted by recent clinical studies^[57]. stated that alpha particles, antimicrobial peptides, chemokines, peroxides and other compounds are released by platelets, all of which have antibacterial effects. Via chemotaxis and immune cell activation, these substances can directly inhibit or destroy pathogens, and also exert indirect antibacterial effects. In the absence of bacterial infection, their various actions can be confirmed by platelet GFs.

CONCLUSION AND RECOMMENDATIONS

BPA at low dose exposures induced deleterious effects on the histological structure of the prostate and disturbed reproductive hormones. Also, this study showed that PRP offers protection against BPA induced prostatic damages in rats. PRP showed significant signs of restoration of the changes in prostate weight and histological with biochemical parameters were improved near to normal. So, this can open a new avenue for the treatment of BPA toxicity in human. Also, we recommended more clinical studies to establish a stronger evidence for effect of PRP on BPA and its analogs induced complications in different organs.

STATEMENT OF ETHICS

All rats received human care in compliance with the guidelines of the Medical Research Ethics Committee of Zagazig University, Egypt (The protocol approval number was ZU-IACUC/3/F/55/2019) and was conformed to the National Institutes of Health guide for the care and use of laboratory animals.

CONFLICT OF INTERESTS

There are No Conflict of Interest.

REFERENCES

1. Skinner, M. K. (2018): Encyclopedia of Reproduction. Academic Press. p309-314.
2. Wu, S.; Huang, D.; Su, X.; Yan, H.; Wu, J. and Sun, Z. (2019): Oral exposure to low-dose bisphenol A induces hyperplasia of dorsolateral prostate and upregulates EGFR expression in adult Sprague-Dawley rats. *Toxicology and Industrial Health*. 35(10):647-659.
3. Ena, L.; Lim, J. S.; Son, J. Y.; Park Y. J.; Lee, Y. H.; Kim, J. Y.; Kwack, S. J.; Lee, B. M.; Ahn, M. Y.; and Kim, H. S. (2018): Evaluation of subchronic exposure to triclosan on hepatorenal and reproductive toxicities in prepubertal male rats. *The Journal of Toxicology & Environmental Health Part A*. 81(11):421-431.
4. Pereira, L. C.; de Souza, A. O.; Bernardes, M. F. F.; Pazin, M.; Tasso, M. J.; Pereira, P. H. and Dorta, D. J. (2015): A perspective on the potential risks of emerging contaminants to human and environmental health. *Environmental Science & Pollution Research*. 22(18):13800-13823.
5. Hormann, A. M., Vom Saal, F. S., Nagel, S. C., Stahlhut, R. W., Moyer, C. L., Ellersieck, M. R., ... & Taylor, J. A. (2014). Holding thermal receipt paper and eating food after using hand sanitizer results in high serum bioactive and urine total levels of bisphenol A (BPA). *PloS one*, 9(10), e110509.
6. Pivnenko, K.; Pedersen, G. A.; Eriksson, E. and Astrup, T. F. (2015): Bisphenol A and its structural analogues in household waste paper. *Waste Management*. 44:39-47.
7. Bonefeld-Jorgensen, E. C.; Long, M.; Hofmeister, M. V. and Vinggaard, A. M. (2007): Endocrine-disrupting potential of bisphenol A, bisphenol A dimethacrylate, 4-n-nonylphenol, and 4-n-octylphenol in *vitro*: new data and a brief review. *Environmental Health Perspective*. 115(1):69-76.
8. Okazaki, H.; Takeda, S.; Kakizoe, K.; Taniguchi, A.; Tokuyasu M.; Himeno, T.; Ishii H.; Kohro-Ikeda, E., Haraguchi, K.; Watanabe, K. and Aramaki, H. (2017): Bisphenol AF as an inducer of estrogen receptor β (ER β): evidence for anti antiestrogenic effects at higher concentrations in human breast cancer cells. *Biological & Pharmaceutical Bulletin*. 40(11):1909-1916.

9. Nadal, A.; Fuentes, E.; Ripoll, C.; Villar-Pazos, S.; Castellano-Muñoz, M.; Soriano, S.; Martinez-Pinna, J.; Quesada, I. and Alonso-Magdalena, P. (2018): Extranuclear-initiated estrogenic actions of endocrine disrupting chemicals: is there toxicology beyond paracelsus?. *The Journal of Steroid Biochemistry & Molecular Biology*. 176:16–22.
10. Alves, R. and Grimalt, R. (2018): A Review of Platelet-Rich Plasma: History, Biology, Mechanism of Action, and Classification. *Skin Appendage Disorders*. 4:18–24.
11. Lynch, M. D. and Bashir, S. (2016): Applications of platelet rich plasma in dermatology: a critical appraisal of the literature. *Journal of Dermatological Treatment*. 27(3):285-289.
12. Girão, L. (2016): PRP and other applications in dermatology; in Alves R, Grimalt R (eds): *Clinical Indications and Treatment Protocols with Platelet-Rich Plasma in Dermatology*. Barcelona, Ediciones Mayo. 73–78.
13. Bigliardi, E.; Cantoni, A. M.; De Cesaris, V.; Denti, L.; Conti, Y.; Bertocchi, M.; Di Ianni, F.; Enrico Parmigiani, E. and Grolli, S. (2018): Use of platelet-rich plasma for the treatment of prostatic cysts in dogs. *The Canadian Journal of Veterinary Research*. 82:264–270
14. Pazzini, J. M.; Nardi, A. B.; Huppel, R.; Gering, A.P.; Ferreira, M.G.;Silveira, C. P. M.; Luzzi, M.C and Santos, R. (2016): Method to obtain platelet-rich plasma from rabbits (*Oryctolagus cuniculus*). *Pesquisa Veterinária Brasileira*. 36(1):39-44.
15. Salem, N.; Hamzaa, A.; Alnahdia, H. and Ayaz, N. (2018): Biochemical and Molecular Mechanisms of Platelet-Rich Plasma in Ameliorating Liver Fibrosis Induced by Dimethylnitrosurea. *Cellular Physiology & Biochemistry*. 47:2331-2339.
16. Gules, O.; Yildiz, M.; Naseer, Z. and Tatar, M. (2019): Effects of folic acid on testicular toxicity induced by bisphenol-A in male Wistar rats. *Biotechnic & Histochemistry*. 94(1):26-35.
17. Karnam, S. S.; Ghosh, R. C.; Mondal, S. and Mondal, M. (2015). Evaluation of subacute bisphenol-A toxicity on male reproductive system. *Veterinary world*, 8(6): 738-744.
18. El-Tahawy, N.F.; Rifaai, R.A.; Saber, E.A.; Saied, S.R. and Ibrahim, R.A. (2017): Effect of Platelet Rich Plasma (PRP) Injection on the Endocrine Pancreas of the Experimentally Induced Diabetes in Male Albino Rats: A Histological and Immunohistochemical Study. *Journal of Diabetes & Metabolism*. 8(3):1-9.
19. Meo, S. A.; Al-Drees, A. M.; Husain, S.; Khan, M. M. and Imran, M. B. (2010): Effects of mobile phone radiation on serum testosterone in Wistar albino rats. *Saudi Medical Journal*. 3(8):869–873.
20. Suvana, S. K.; Layton, C. and Bancroft, J. D. (2019): *Bancroft's theory and practice of histological techniques*. 8th ed., New York, London: Churchill Livingstone.
21. Singh, D. (2003): Principle and Technique. In *Histology, Microscopy and Photography*. 1st ed., CBS Publishers and Distributes. New Delhi, Bangalore (India). Pp: 679-699
22. Taylor, C. R. and Rudbeck, L. (2013): *Immunohistochemical Staining Methods*. 6th ed., Chapter 6 edited by Petersen, K. and Pedersen, H.C. Dako Denmark A/S, An Agilent Technologies Company.
23. Dean, A.; Dean, G. and Colombier, D. (2000): *Epi-info version 1 for the year 2000 data basic statics and epidemiology on microcomputer* CDC. Georgia, USA.
24. Cariati, F.; D'Uonno, N.; Borrillo, F.; Iervolino, S.; Galdiero, G. and Tomaiuolo, R. (2019): "Bisphenol a: an emerging threat to male fertility". *Reproductive Biology & Endocrinology*. 17(6):1-8.
25. Ullah, A; Pirzada, M.; Afsar, T.; Razak, S.; Almajwal, A. and Jahan, S. (2019): Effect of bisphenol F, an analog of bisphenol A, on the reproductive functions of male rats. *Environmental Health & Preventive Medicine*. 24(41):1-11.
26. Yousaf, B.; Liu, G.; Wang, R.; Qadir, A., Ali, M. U.; Qudisia Kanwal, Q.; Munir, B. and Abbas, Z. (2016): Bisphenol A exposure and healing effects of *Adiantum capillus-veneris* L. plant extract (APE) in bisphenol A-induced reproductive toxicity in albino rats. *Environmental Science & Pollution Research*. 23(12):11645–11657.
27. Johnson, S. A.; Spollen, W. G.; Manshack, L. K.; Bivens, N. J.; Givan, S. A. and Rosenfeld, C. S. (2017): Hypothalamic transcriptomic alterations in male and female California mice (*Peromyscus californicus*) developmentally exposed to bisphenol A or ethinyl estradiol. *Physical Reports*. 5(3): e13133.
28. Jin, P.; Wang, X.; Chang, F.; Bai, Y.; Li, Y.; Zhou, R. and Chen, L. (2013): Low dose bisphenol A impairs spermatogenesis by suppressing reproductive hormone production and promoting germ cell apoptosis in adult rats. *Journal of Biomedical Research*. 27(2): 135–144.
29. Zhang, M.; Lin, Q.; Qi, T.; Wang, T.; Chen, C.; Riggs, A.D. and Zeng, D. (2016): Growth factors and medium hyperglycemia induce Sox9+ ductal cell differentiation into β cells in mice with reversal of diabetes. *Proceedings of the National Academy of Sciences*. 113(3): 650-655.
30. Huang, D. Y.; Zheng, C.C.; Pan, Q.; Wu, S.S.; , Xin Su, Li, L.; Wu, J.H. and Sun, Z.Y. (2018): Oral exposure of low-dose bisphenol A promotes proliferation of dorsolateral prostate and induces epithelial–mesenchymal transition in aged rats. *Scientific Reports*. 8(490):1-10.

31. Nakamura, D.; Yanagiba, Y.; Duan, Z.; Ito, Y.; Okamura, A.; Asaeda, N.; Tagawa, Y.; Li, C.; Taya, K.; Zhang, S. Y.; Naito, H.; Ramdhan, D. H.; Kamijima, M. and Nakajima, T. (2010): Bisphenol A may cause testosterone reduction by adversely affecting both testis and pituitary systems similar to estradiol. *Toxicology Letters*. 194(1-2):16–25.
32. Eid, J. I.; Eissa, S. M. and El-Ghor, A. A. (2015): Bisphenol A induces oxidative stress and DNA damage in hepatic tissue of female rat offspring. *The Journal of Basic & Applied Zoology*. 71:10-19.
33. Tolba, A. and Mandour, D.A. (2018): Histological effects of bisphenol-A on the reproductive organs of the adult male albino rat. *European Journal of Anatomy*. 22 (2): 89-102.
34. Shaimaa, H. A. (2019): Histopathological Changes Produced by Bisphenol A in the Renal Cortex of Adult Male Albino Rats. *The Medical Journal of Cairo University*. 87(3):2045-2058.
35. De Souza, D. A., Borges, A. C.; Santana, A. C.; Oliver, C., and Jamur, M. C. (2015): Mast cell proteases 6 and 7 stimulate angiogenesis by inducing endothelial cells to release angiogenic factors. *PLoS One*, 10(12), e0144081.
36. Fairweather, D. and Frisancho-Kiss, S. (2008): Mast cells and inflammatory heart disease: potential drug targets. *Cardiovascular & Haematological Disorders-Drug Targets (Formerly Current Drug Targets-Cardiovascular & Hematological Disorders)*. 8(1): 80-90.
37. Hu, Y.; Zhang, L.; Wu, X.; Hou, L.; Li, Z.; Ju, J. and Zhou, T. (2016): Bisphenol A, an environmental estrogen-like toxic chemical, induces cardiac fibrosis by activating the ERK1/2 pathway. *Toxicology Letters*. 250:1-9.
38. Manal, M. M., & Ibrahim, H. I. (2019). Hazards of Bisphenol A on the Thyroid Gland of Adult Male Albino Rats and Possibility of Recovery after its Withdrawal. *The Medical Journal of Cairo University*, 87(September), 2945-2953.
39. Alboghobeish, S.; Mahdavinia, M.; Zeidooni, L.; Samimi, A.; Oroojan, A. A.; Alizadeh, S. and Khorsandi, L. (2019): Efficiency of naringin against reproductive toxicity and testicular damages induced by bisphenol A in rats. *Iranian Journal of Basic Medical Sciences*. 22(3): 315-323.
40. Yang, Y.; Hu, S.; Liu, J.; YunCui, Y.; Fan, Y.; Lv, T.; Liu, L.; Li, J.; He, Q.; Han, W.; Yu, W.; Sun, Y. and Jin, J. (2017): CD8⁺ T cells promote proliferation of benign prostatic hyperplasia epithelial cells under low androgen level via modulation of CCL5/ STAT5/ CCND1 signaling pathway. *Scientific Reports*. 7:1-12.
41. Ou, Z.; He, Y.; Qi, L.; Zu, X.; Wu, L.; Cao, Z.; Li, Y.; Liu, L.; Dube, D. A.; Wang, Z. and Wang, L. (2017): Infiltrating mast cells enhance benign prostatic hyperplasia through IL-6/STAT3/Cyclin D1 signals. *Oncotarget*. 8(35): 59156-59164.
42. Archana, M.; Yogesh, T. L. and Kumaraswamy, K. L. (2013): Various methods available for detection of apoptotic cells-A review. *Indian Journal of Cancer*. 50 (3): 274-283.
43. Mokra, K.; Kocia, M. and Michałowicz, J. (2015): Bisphenol A and its analogs exhibit different apoptotic potential in peripheral blood mononuclear cells (in *vitro* study). *Food & Chemical Toxicology*. 84: 79-88.
44. Walker, M. M.; Ellis, S. M.; Auza, M. J.; Patel, A. and Clark, P. (2008): The intercellular adhesion molecule, cadherin-10, is a marker for human prostate luminal epithelial cells that is not expressed in prostate cancer. *Modern Pathology*. 21(2):85-95.
45. Robbins, S. L.; Cortan, R. S. and Kumar, V. (2011): *Pathologic basis of disease*. 9th ed.: WB Saunders Company, Canada.
46. Hasanluyi, E. A.; Banan Khojasteh, S. M. and Nejhad, D. M. (2016): Investigation of the effects of Bisphenol A on the histology and ultrastructure of prostate and seminal vesicle glands in rats. *Thrita*. 5(4): 1-7.
47. Marshall, C. B. (2016): Rethinking glomerular basement membrane thickening in diabetic nephropathy: adaptive or pathogenic?. *American Journal of Physiology-Renal Physiology*, 311(5), F831-F843.
48. Yoon, J.; Bang, S. H.; Park, J. S.; Chang, S. T.; Kim, Y. H., & Min, J. (2011): Increased in *vitro* lysosomal function in oxidative stress-induced cell lines. *Applied biochemistry and biotechnology*, 163(8), 1002-1011.
49. El-Rouby N. M. (2010): A Histological study on the effect of diclofenac sodium (declophen) administration on thyroid follicular cells of albino rats. *Egyptian Journal of Histology*. 33(2): 213-223.
50. Huang, D.; Wu, J.; Su, X.; Yan, H. and Sun, Z. (2017): Effects of low dose of bisphenol A on the proliferation and mechanism of primary cultured prostate epithelial cells in rodents. *Oncology Letters*. 14(3):2635-2642.
51. Vandenberg, L. N.; Chahoud, I.; Heindel, J. J.; Padmanabhan, V.; Paumgarten, F. J. and Schoenfelder, G. (2010): Urinary, circulating, and tissue biomonitoring studies indicate widespread exposure to bisphenol A. *Environmental Health Perspective*. 118:1055–1070.
52. Rah, D. K.; Min, H. J.; Kim, Y. W. and Cheon, Y. W. (2017): Effect of Platelet-Rich Plasma on Ischemia-Reperfusion Injury in a Skin Flap Mouse Model. *International Journal of Medical Sciences*. 14(9):829–839.

53. Esat, D. M.; Temel, S.; Ozer, H.; Kemal, U. M.; Kaya, F.; Aslan, F. and Kismet, K. (2016): Comparison of the Effects of Platelet rich Plasma Prepared in Various Forms on the Healing of Dermal Wounds in Rats. *Wounds: a compendium of clinical research and practice*, 28(3), 99-108.
54. Jia, C.; Lu, Y.; Bo Bi, Chen, L.; Yang, Q.; Yang, P.; Guo, Y. Zhu, J.; Zhu, N. and Liu, T. (2017): Platelet-rich plasma ameliorates senescence-like phenotypes in a cellular photoaging model. *RSC Advances*. 7:3152–3160.
55. Martini, L.; Via, A. G.; Fossati, C.; Randelli, F.; Randelli, P. and Cucchi, D. (2017): Single Platelet-Rich Plasma Injection for Early Stage of Osteoarthritis of the Knee. *Joints*. 5 (1):2-6.
56. Jang, H. Y.; Myoung, S. M.; Choe, J. M.; Kim, T.; Cheon, Y. P.; Kim, Y. M. and Park, H. (2017): Effects of Autologous Platelet-Rich Plasma on Regeneration of Damaged Endometrium in Female Rats. *Yonsei Medical Journal*. 58 (6):1195-1203.
57. Li, T.; Ma, Y.; Wang, M.; Wang, T.; Wei, J.; Ren, R.; He, M.; Wang, G.; Boey, J.; Armstrong, D. G.; Deng, W. and Chen, B. (2019): Platelet-rich plasma plays an antibacterial, anti-inflammatory and cell proliferation-promoting role in an *in vitro* model for diabetic infected wounds. *Infection & Drug Resistance*. 12:297-309.

الملخص العربي

التأثير المحسن للبلازما الغنية بالصفائح الدموية على التغييرات الهستولوجية و البيوكيميائية التي أحدثها بيسفينول-أ في غده البروستاتا للجرذان المهق البالغين

نهله السيد ابراهيم، ايه علاء الدين محمود، عصماء عثمان سليم، سالي احمد سليم

قسم الهستولوجيا الطبيه وبيولوجيا الخلية بكلية الطب البشري جامعه الزقازيق مصر

المقدمه: ادت زياده المواد الكيميائية البيئي الطبيعيه والصناعية المعروفة باسم المواد الكيميائية المعطلة للغدد الصماء الى حدوث اضطرابات تناسلية للذكور على مستوى متصاعد مما جعل هذه المواد تكتسب اهتماما فى علم وظائف الاعضاء البشرية والدراسات الضخمة التي تهدف إلى شرح كيفية تأثير هذه المواد الكيميائية على نظام الغدد الصماء. واحدة من هذه المواد هو البيسفينول أ يتم. استخدامه على نطاق واسع في منتجات مختلفة من الحياة اليومية. البلازما الغنية بالصفائح الدموية هي مجال ناشئ في معالجة الجوانب المختلفة عن طريق تحسين و تجديد الانسجة عن طريق إطلاق عوامل النمو والسيوتوكينات.

الهدف من البحث: تقييم التأثير العلاجي للبلازما الغنية بالصفائح الدموية ضد أمراض البروستاتا التي يسببها البيسفينول أ في ذكور الجرذان البيضاء

المواد والطرق: تم استخدام خمسة وثلاثين من ذكور الجرذان البيضاء البالغة قسمت إلى ثلاث مجموعات: المجموعة الأولى: التي عملت كمجموعة تحكم المجموعة الثانية: تم حقنهم بواسطة البيسفينول أ ٥٠ مجم /كجم يوميا لمدة ٤ اسابيع. المجموعة الثالثة: تم حقنهم بالبيسفينول أ كما فى المجموعة الثانية لمدة ٤ اسابيع ثم تم حقنهم ب ٥ مل من البلازما الغنية بالصفائح الدموية المذابة فى كميته مساوية من مالح الفوسفات مرتين اسبوعيا لمدة ٤ اسابيع تحت الجلد ثم تعرضت الفئران من جميع المجموعات لما يلي ؛ تحليل كيميائي حيوي لهرمون التستوستيرون فى الدم ، دراسات كيميائية مناعية لمستقبلات الاندروجين والاستروجين وفحص المجهر الضوئي والالكتروني.

النتائج: فيما يتعلق بمستويات هرمون التستوستيرون ، كان هناك انخفاض كبير للغاية المجموعة الثانية عند مقارنتها أيضا بالمجموعات الاخرى. كشف الفحص وفره ألياف الكولاجين البارزة والاعوية الدموية المزدهمة بالخلايا البدنية والتسلل الخلوي الالتهابي.. كما أظهر العديد من أسيني المناطق البؤرية انتشار الظهارة أو التقسيم الطبقي. تقريبا كل هذه الخلايا الظهارية أوضحت الانماط النووية المختلفة. شاحب أو حويصلي ، داكن ، غير منتظم مع رغوي قمي أو سيتوبالزم مفرغ. أيضا ، كما ظهرت العديد من الخلايا القاعدية ذات النوى المسطحة أو الثالثة أو المطولة بشكل داكن بسهولة وقد لوحظ العديد من الشعيرات الدموية المخترقة فى الاشكال الظهارية المختلفة. أيضا و شوهدت الخلايا المنفصلة ذات النوى غير المنتظمة والاجسام السيتوبلازمية فى عدة لومينات أسيني. أظهرت ايضا المجموعة التي عولجت بالبيسفينول- أن جميع الخلايا تقريبا لمستقبلات الاندروجين ذات رد فعل نووي سلبي ولكن لا تزال بعض الخلايا ايجابية. بينما أظهر الكشف عن مستقبلات الاستروجين رد فعل ايجابي قوي فى نوى العديد من الخلايا القاعدية. أما فيما يخص الفحص بالميكروسكوب الالكترونى ، فقد شوهدت تقريبا جميع الخلايا الافرازية لديها نوى غير متجانسة غير منتظمة أو ذات مسافة بادئة ، صهاريح متوسعة بشكل معتدل وواسع النطاق من الشبكة الاندوبلازمية الخشنة ، متناثرة قمية قليلة الحبيبات الدقيقة. بينما أظهرت الخلايا القاعدية نوى غير متجانسة مسطحة أو طويلة. بالإضافة إلى ذلك، أظهرت العديد من الوحدات الافرازية فى مناطق التركيز للطبقات كانت خلاياهم تحتوي على نوى ذات شكل

غير منتظم مع صهاريج متوسعة غير منتظمة من الشبكة الاندوبلازمية الخشنة ، والعديد من الاوعية الدقيقة المتجمعة، والجسيمات الليمفاوية متعددة الاشكال والخلايا ولكن بعد إعطاء البلازما الغنية بالصفائح الدموية اظهرت تحسنا في العديد من هذه التغييرات.

الخلاصة: أظهرت نتائج دراستنا الحالية أن البيسفينول بجرعات منخفضة قد يكون لها نتائج ضارة على البنية النسيجية للبروستاتا والهرمونات التناسلية المضطربة. كما أظهرت هذه الدراسة أن للبلازما الغنية بالصفائح الدموية دور في حماية البروستاتا ضد الاضرار التي يسببها البيسفينول أ